

## Thermal properties of bulk polyimides: insights from computer modeling *versus* experiment

Cite this: *Soft Matter*, 2014, 10, 1224

Sergey V. Lyulin,<sup>ab</sup> Sergey V. Larin,<sup>a</sup> Andrey A. Gurtovenko,<sup>ab</sup> Victor M. Nazarychev,<sup>a</sup> Stanislav G. Falkovich,<sup>ab</sup> Vladimir E. Yudin,<sup>a</sup> Valentin M. Svetlichnyi,<sup>a</sup> Iosif V. Gofman<sup>a</sup> and Alexey V. Lyulin<sup>\*c</sup>

Due to the great importance for many industrial applications it is crucial from the point of view of theoretical description to reproduce thermal properties of thermoplastic polyimides as accurate as possible in order to establish "chemical structure–physical properties" relationships of new materials. In this paper we employ differential scanning calorimetry, dilatometry, and atomistic molecular dynamics (MD) simulations to explore whether the state-of-the-art computer modeling can serve as a precise tool for probing thermal properties of polyimides with highly polar groups. For this purpose the polyimide R–BAPS based on dianhydride 1,3-bis(3',4'-dicarboxyphenoxy)benzene (dianhydride R) and diamine 4,4'-bis(4''-aminophenoxy)biphenyl sulphone (diamine BAPS) was synthesized and extensively studied. Overall, our findings show that the widely used glass-transition temperature  $T_g$  evaluated from MD simulations should be employed with great caution for verification of the polyimide computational models against experimental data: in addition to the well-known impact of the cooling rate on the glass-transition temperature, correct definition of  $T_g$  requires cooling that starts from very high temperatures (no less than 800 K for considered polyimides) and accurate evaluation of the appropriate cooling rate, otherwise the errors in the measured values of  $T_g$  become undefined. In contrast to the glass-transition temperature, the volumetric coefficient of thermal expansion (CTE) does not depend on the cooling rate in the low-temperature domain ( $T < T_g$ ) so that comparison of computational and experimental values of CTE provides a much safer way for proper validation of the theoretical model when electrostatic interactions are taken into account explicitly. Remarkably, this conclusion is most likely of generic nature: we show that it also holds for the commercial polyimide EXTEM<sup>TM</sup>, another polyimide with a similar chemical structure.

Received 26th September 2013  
Accepted 5th December 2013

DOI: 10.1039/c3sm52521j

www.rsc.org/softmatter

### Introduction

Computer-aided design is often considered nowadays as a means for development of novel materials with pre-defined characteristics. A starting point for such design is the availability of high-quality computational models that are extensively verified against experimental data. In other words, to develop new materials *in silico* one has to reproduce first the properties of existing ones.

In this study we focus on thermoplastic polyimides, an important class of heat-resistant polymers, which can be used for numerous industrial applications including manufacturing of composite materials for the aerospace industry. Because of their importance, the polyimides have extensively been studied

experimentally;<sup>1–4</sup> they have also been a subject of many computational studies.<sup>5–29</sup> Most of the computational studies addressed the transport properties of PIs<sup>5–22,24,25</sup> *via* probing the diffusion of small molecules through polyimide membranes. We note however that great attention to thermoplastic polyimide-based materials has been attracted largely due to their excellent heat-resistant properties.<sup>1</sup> It is therefore crucial for any computational model of polyimides to reproduce polyimide's thermal properties as accurate as possible.

The problem of the correct determination of thermal properties from computer simulations exists for virtually all glass-forming heterocyclic polymers. Overall, atomistic computer modeling of polymers in bulk is a well-developed area; see *e.g.* ref. [30–32] for an overview. By far most computational studies have focused mainly on polymers with a relatively simple chemical structure such as polyethylene and polystyrene;<sup>33,34</sup> polyimides have been studied to a considerably lesser extent. The protocol for evaluating thermal properties with the use of computer simulations is similar for the majority of polymers studied. First, an equilibrated polymer sample is prepared

<sup>a</sup>Institute of Macromolecular Compounds, Russian Academy of Sciences, Bol'shoi pr. 31 (V.O.), St. Petersburg, 199004 Russia

<sup>b</sup>Department of Physics, St. Petersburg State University, Ulyanovskaya str. 1, Petrodvorets, St. Petersburg, 198504 Russia

<sup>c</sup>Theory of Polymers and Soft Matter Group, Technische Universiteit Eindhoven, PO Box 513, 5600 MB Eindhoven, The Netherlands. E-mail: a.v.lyulin@tue.nl

through simulation of the system at elevated temperatures that are well above the glass-transition temperature. The equilibrated sample is then cooled down until the room temperature has been reached and the thermal properties (such as the glass transition temperature,  $T_g$ , which exceeds significantly room temperature in the case of polyimides) are calculated.<sup>21–23,25,27,28,30,35–40</sup> However, the subsequent comparison of the calculated values of  $T_g$  with experimental data is not straightforward due to an enormous difference (up to 10–15 orders of magnitude) in the cooling rates employed in computer simulations and experiments.<sup>21–23,25,27,28,37,40</sup> Computer modeling normally overestimates the glass-transition temperature due to extremely high cooling rates because of which one should employ some empirical logarithmic corrections before making a comparison with the experiment.<sup>29,36,39,41</sup> Unfortunately, such corrections are polymer-specific; extracting the corresponding dependence of the glass-transition temperature on the cooling rate requires extensive simulation efforts: to get just a few data points on the logarithmic “ $T_g$  – cooling rate” curve implies an increase in the required simulation time by several orders of magnitude.

In this paper we employ differential scanning calorimetry (DSC), dilatometry, and atomic-scale molecular-dynamics (MD) simulations to explore whether the state-of-the-art computer modeling can serve as a precise tool for probing thermal properties of polyimides. For our study the polyimide R-BAPS (based on R dianhydride 1,3-bis(3',4-dicarboxyphenoxy)benzene and diamine BAPS 4,4'-bis(4''-aminophenoxy)biphenyl sulphone) was synthesized, see Fig. 1 for the chemical structure of its monomer unit. From the point of view of theoretical description the atomistic computer modeling of this polyimide is challenging: due to an oxidized sulphone group in its monomer unit the partial atomic charges of the polymer are far from zero and cannot be neglected. This is in contrast to *e.g.* polystyrene that has rather small and therefore negligible partial charges. The presence of strong intermolecular electrostatic interactions considerably slows down local dynamics of a polymer in the bulk, so proper equilibration of the polymer sample can require enormous computational efforts. Furthermore, modification of a polyimide diamine fragment by adding such polar groups leads to significant improvement of its thermal properties as is seen from experiments.<sup>3,4,6,38,42</sup>

Overall, our results indicate that the glass-transition temperature  $T_g$  evaluated from computer modeling should be used with caution for verification of the computational model of a bulk polymer against experimental data, especially for the systems in which electrostatic interactions play a crucial role. The main reason for this conclusion is that the slope of the density–temperature curve in the high-temperature domain ( $T > T_g$ ) may be very sensitive to the cooling rates accessible for simulations, making additional errors in the evaluation of  $T_g$  undefined. In contrast to the glass-transition temperature, the volumetric thermal expansion coefficient (CTE) does not depend on the cooling rate at the temperatures  $T < T_g$ . Therefore, to validate the theoretical model the CTE would be much more preferable. Remarkably, this conclusion is also confirmed for the commercial polyimide EXTEM™, another polyimide with a sulphone group in the monomer unit, see Fig. 1.

## Methods

### Experimental methods

Polyamic acid (PAA) was obtained by polycondensation of 1,3-bis(3',4-dicarboxyphenoxy)benzene (R) and 4,4'-bis(4''-aminophenoxy)diphenylsulphone (BAPS) in 20 wt% solution of *N*-methyl-2-pyrrolidone (NMP) at 25 °C. Diamine BAPS was supplied by Wakayama Seika Co., Ltd. (Japan).

A series of polyimides with different molecular weights was synthesized by controlling the ratio of monomers to the end-capper (phthalic anhydride PA). Molecular-weight control was promoted through stoichiometric offset of the monomers (dianhydride, diamine and phthalic anhydride) according to the Carothers relationship. The polyamic acids (R-BAPS-PA) were converted to their respective polyimides by using solution imidization techniques. An azeotropic liquid, toluene, was added to PAA solution to achieve 80/20 ratio of NMP to toluene, and stirred at about 180 °C in a nitrogen atmosphere. After about five hours of the azeotropic distillation of by-product water, yellow-brown highly viscous solution of PI with PA end groups is obtained. After cooling down to room temperature the PI solution is diluted with NMP, added slowly into the vessel with alcohol and stirred vigorously. The produced white powder was filtered, washed with water, and dried in a vacuum oven at

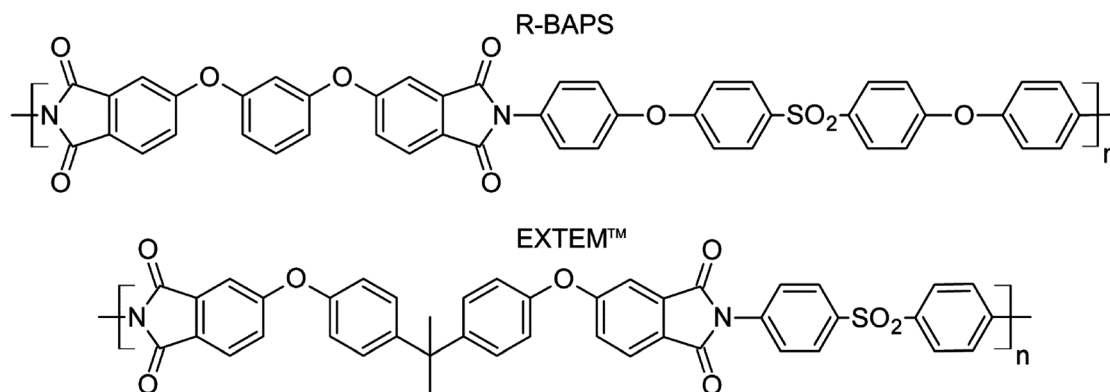


Fig. 1 The chemical structure of monomer units of polyimides R-BAPS and EXTEM™.

200 °C overnight and subsequently at 250 °C for two hours to ensure complete imidization. The standard infra-red spectroscopy was used to confirm the formation of polyimides *via* the characteristic absorption peaks at 1780 cm<sup>-1</sup>, 1720 cm<sup>-1</sup>, 1380 cm<sup>-1</sup>, and 725 cm<sup>-1</sup> that are typical for aromatic PIs.

Polymer molecular weights  $M_n$  have been determined by size-exclusion chromatography (SEC) in DMF at a flow rate of 1.0 mL min<sup>-1</sup> and at temperature  $T = 40$  °C. The system was comprised of a Waters 515 HPLC pump, a Waters 2410 RI detector, a Waters 2457 Dual I absorbance detector, a column oven, and a PolymerLabs PLgel 5 mm MIXED-C 300 × 7.5 mm column. The column was calibrated with a series of narrow molecular-weight distribution poly(methyl methacrylate)s using PolymerLabs standards.

Differential scanning calorimetry (DSC) measurements have been performed to estimate the glass-transition temperature  $T_g$  of the series of polyimides with different molecular weights by using 3–6 mg samples contained in a platinum crucible with a heating velocity of 10 °C min<sup>-1</sup> in a nitrogen atmosphere.

To measure the coefficient of linear thermal expansion, CLTE, the cylindrical sample of the R-BAPS polyimide with the maximal value of  $M_n$  has been prepared by hot pressing of R-BAPS powder at  $T = 300$  °C with the use of a compressive pressure of 600 MPa. The sample was subsequently cooled down to room temperature in the press-mould under the same pressure. The diameter and the height of the sample amounted to 10 and 30 mm, respectively. In order to dissipate the residual mechanical stress the sample was annealed by heating up to 205 °C in the unloaded state.

To control the quality of the polyimide sample, the density of the material has been refined by the floatation method. The mixtures of toluene and carbon tetrachloride were used for this test. The obtained value of the density,  $1.365 \pm 0.002$  g cm<sup>-3</sup>, was in agreement with that measured in previous studies.<sup>4</sup>

The CLTE measurements have been carried out by linear dilatometry using a TMA Q400 (TA Instruments, USA) thermo-mechanical analyzer. The cylindrical sample was heated from 20 °C to 205 °C with a heating rate of 5 deg min<sup>-1</sup>; a small, ~120 Pa, constant compressive load was applied to the flat ends of the sample. During the CLTE tests the changes in the sample length due to temperature variation were monitored. In the case of isotropic samples, the temperature dependence of the volumetric coefficient of temperature expansion, CTE, was simply recalculated from the experimental values of CLTE ( $CTE = 3 \times CLTE$ ).

### Computer simulation methods

Bulk samples of heat-resistant polyimides R-BAPS and EXTEM<sup>TM</sup>, Fig. 1, have been studied through atomic-scale molecular-dynamics (MD) simulations. Both polymer systems are comprised of 27 polyimide chains. Each R-BAPS chain consists of eight monomer units; such chains are shown to be long enough to eliminate the influence of the molecular weight of chains on the thermal properties of samples (see next section). In turn, each EXTEM<sup>TM</sup> chain consists of nine monomer units, ensuring that the molecular weights of R-BAPS and

EXTEM<sup>TM</sup> chains are approximately the same. The total number of atoms in the polyimide samples was around 18 400 (for R-BAPS) or 20 000 (for EXTEM<sup>TM</sup>). The atomistic force-field GROMOS96 (ref. 43) was used for both R-BAPS and EXTEM<sup>TM</sup> polyimides. To evaluate partial charges the Firefly package<sup>44</sup> was used to perform the Hartree-Fock (HF) calculations on a polyimide monomer unit at the 6-31G\* level, the charges were assigned by the Mulliken method.<sup>42</sup> We note that both R-BAPS and EXTEM<sup>TM</sup> monomer units have relatively large partial charges due to the presence of sulphone groups. The Lennard-Jones interactions were cut off at 1 nm. The particle-mesh Ewald method was used to handle the long-range electrostatic interactions.<sup>45,46</sup> All bond lengths were kept constant with the LINCS algorithm.<sup>47</sup> The simulations were performed in the NpT ensemble. The Berendsen thermostat and barostat were employed to control the temperature and pressure, respectively.<sup>48</sup> The time step was set to 2 fs. Energy conservation was confirmed through additional short simulations in the NVE ensemble. All simulations were performed with the use of the GROMACS simulation suite<sup>43,49,50</sup> on the Lomonosov super-computer (computational facilities of Moscow State University, 38-th place in top-100 world ranking). Typical simulation runs employ 48 CPU cores. The total simulated time exceeded 25 microseconds which corresponded to about 480 000 CPU·hours (approx. 55 CPU·years).

To generate initial polymer melt samples different methods have been reported in the literature, which include various Monte-Carlo schemes, coarse-grained approaches with follow-up reverse-mapping procedures and direct simulations of polymerization reactions.<sup>51–54</sup> However, for heterocyclic polymers some of these protocols<sup>8,12,21</sup> may produce various artifacts related to concatenation of phenyl rings and side groups and require generation of initial structures at very low densities (around 10% of the target values) and subsequent compression at extremely high pressure (several tens of thousands of bars). An atomistic single-chain sampling generation procedure that combines pivot Monte Carlo moves for rotatable torsions and standard MD algorithms to explore various oscillatory modes of chains has been developed in ref. [20]; the method allows one to generate equilibrium melt structures at given temperature. However, in all the approaches mentioned it is the density which is used to monitor the system equilibration<sup>8,12,15,21,25</sup> which may be inaccurate as shown in our previous work.<sup>42</sup>

In this study preparation of a polyimide sample was performed at an elevated temperature ( $T = 600$  K) and followed closely by a two-step procedure described in detail in the preceding publication.<sup>42</sup> Briefly, the basic idea was to decrease (by about two orders of magnitude) the equilibration time by switching off strong intra- and intermolecular electrostatic interactions in the system. As a first step, after compression (with the maximum value being around 300 bar only) and annealing of an initially “gaseous” polyimide sample, the system was simulated for 3 microseconds with the partial charges switched off. As shown,<sup>42,55</sup> full equilibration for the polyimide of the chosen molecular weight requires ~1.5 μs. Therefore, first 2 microseconds of simulations were considered as the equilibration period. The third microsecond of MD

simulations was used for preparation of 11 polyimide samples which were taken from the microsecond MD trajectory every 100 ns. As a second step of the procedure, the partial charges were switched on and each sample with full electrostatics was further equilibrated for 100 ns. This time span was shown to be one order of magnitude higher than typical relaxation times in the system under study (the relaxation times of autocorrelation functions for the density<sup>38</sup> of the system and for the end-to-end chain vector were estimated to be less than 10 ns). Therefore, a 100 ns time span is proved to be long enough for proper equilibration after switching electrostatics on.<sup>42</sup>

The prepared sets of samples (both samples with and without partial charges) were used for the investigation of thermal properties. The samples with partial charges switched off were cooled down with five different cooling rates to room temperature. The corresponding density–temperature curves were used then for evaluating the glass transition temperature and the volumetric thermal expansion coefficient; both thermal characteristics were averaged over all the 11 polyimide samples. To get insight into the influence of long-range electrostatic interactions, we chose one of the cooling rates considered and repeated the same measurements of the thermal properties for the polyimide samples with full electrostatics.

## Results

### The static structure factor

In order to explore the structure of the considered R–BAPS samples at different temperatures with and without electrostatic interactions, we calculated the static structure factor  $S(q)$ , Fig. 2, in addition to the radius of gyration reported in our recent publication.<sup>42</sup>

As can be followed from Fig. 2, switching on the electrostatic interactions does not lead to significant change in the polyimide structure both at low (290 K) and at high (600 K) temperatures. Furthermore, the positions of the pronounced first peak and also of the second peak are very similar to what is expected for other polymers, *e.g.* polystyrene.<sup>56</sup>

### The glass-transition temperature

The glass transition temperature of a series of R–BAPS polyimide samples of various molecular weights was measured by DSC. The results are presented in Fig. 3. It is seen that the glass transition temperature  $T_g$  for relatively short chains increases with molecular weight (oligomer-like behavior), while there is no change in the glass transition temperature for longer chains (polymer-like behavior). Such a molecular-weight dependence of  $T_g$  can often be described by the well-known Fox–Flory's law<sup>57</sup>

$$T_g = T_{g0} - K/M_n \quad (1)$$

where  $T_{g0}$  is the glass transition temperature of a polymer with infinite molecular weight,  $K$  is an empirical parameter and  $M_n$  is the number-average molecular weight. Indeed, the experimental data presented in Fig. 3 can be fitted very well with the use of eqn (1) and the following set of parameters:  $T_{g0} = 222$  °C and  $K = 80$  °C kg mol<sup>−1</sup>. The beginning of the polymer-like behavior can be identified from Fig. 3 as  $M_n \sim 6$  kg mol<sup>−1</sup>.

In other words, starting from the value of  $M_n \sim 6$  kg mol<sup>−1</sup> further increase in the number-average molecular weight of R–BAPS polyimides leads to the increase in  $T_g$  by less than 15–18 degrees, which is comparable with typical errors in calculation of  $T_g$  from simulation data.<sup>42</sup>

The experimental results for the glass transition temperature of the R–BAPS polyimide can now be used for setting up a

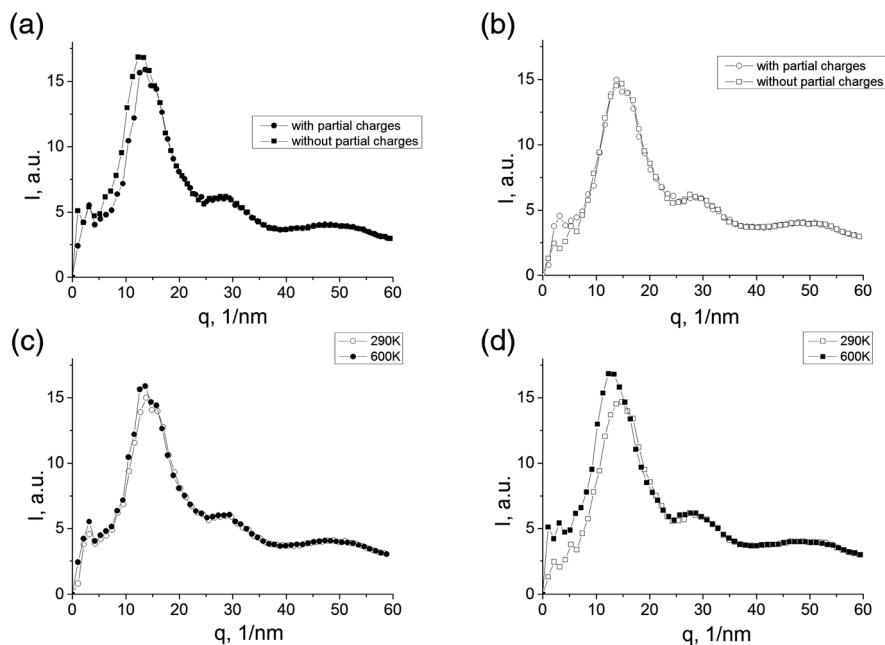


Fig. 2 The static structure factor  $S(q)$  for the R–BAPS polyimide at temperatures 600 K (a) and 290 K (b) with (c) and without (d) partial charges.



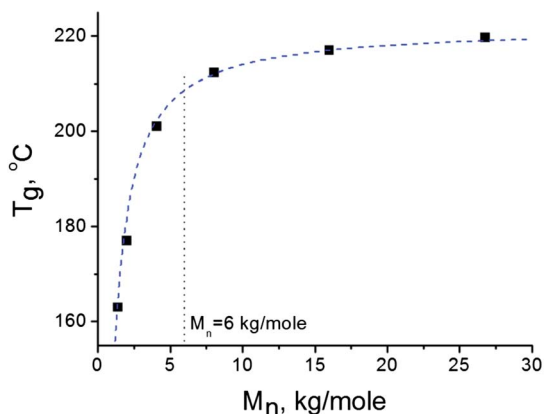


Fig. 3 The glass transition temperature of a series of R-BAPS polyimide samples *versus* the number-average molecular weight of a polymer as measured by differential scanning calorimetry. Also shown are the fit to the Fox-Flory law (dashed line) and the beginning of the polymer-like behavior (vertical dotted line).

polymer sample to be studied in atomistic computer modeling. To make molecular-dynamics (MD) simulations as efficient as possible one should consider relatively short chains as this speeds up polymer sample equilibration. On the other hand, the polymer chains cannot be too short to eliminate sensitivity of polymer's thermal properties to the molecular weight. According to Fig. 3, the polymer-like behavior starts at  $M_n \sim 6$  kg mol<sup>-1</sup>, because of which we chose the chain length in simulations to be 8 monomer units (this degree of polymerization corresponds to  $M_n \sim 6.4$  kg mol<sup>-1</sup>). In addition, with use of the virtual bond model<sup>58–61</sup> we also estimated that the value of the Kuhn segment for the R-BAPS polyimide is around 1 nm which is close to the Kuhn segment calculated previously by the AM1 method.<sup>58</sup> The calculated value of the Kuhn segment implies that a polyimide chain of 8 monomer units consists of  $\sim 18$  Kuhn segments and can therefore be considered as a Gaussian chain. This provides further support for the chosen length of R-BAPS chains to be used in simulations and for the polymer-like behavior of the corresponding polymer samples.

For the R-BAPS polyimide of the chosen molecular weight we have performed microsecond atomic-scale molecular dynamics simulations and evaluated the glass transition temperature, see “Computer simulation methods” section for details. To estimate the influence of the cooling rate on the glass transition temperature, 11 well-equilibrated polyimide samples with partial charges switched off were cooled down stepwise from 600 K to 290 K with five different cooling rates.

The cooling rates ranged from  $\gamma = 1.5 \times 10^{14}$  K min<sup>-1</sup> (4 ps of MD simulations for each 10 K temperature step) to  $\gamma = 1.5 \times 10^{10}$  K min<sup>-1</sup> (40 ns of MD simulations for each 10 K step, amounting to 1.28  $\mu$ s of MD simulations for a single sample or to  $\sim 14$   $\mu$ s-long simulations for all the samples). The corresponding “density-temperature” curves for different cooling rates are presented in Fig. 4a (all curves were averaged over 11 samples).

The experimental value of the glass transition temperature for the R-BAPS polyimide of the same molecular weight as that

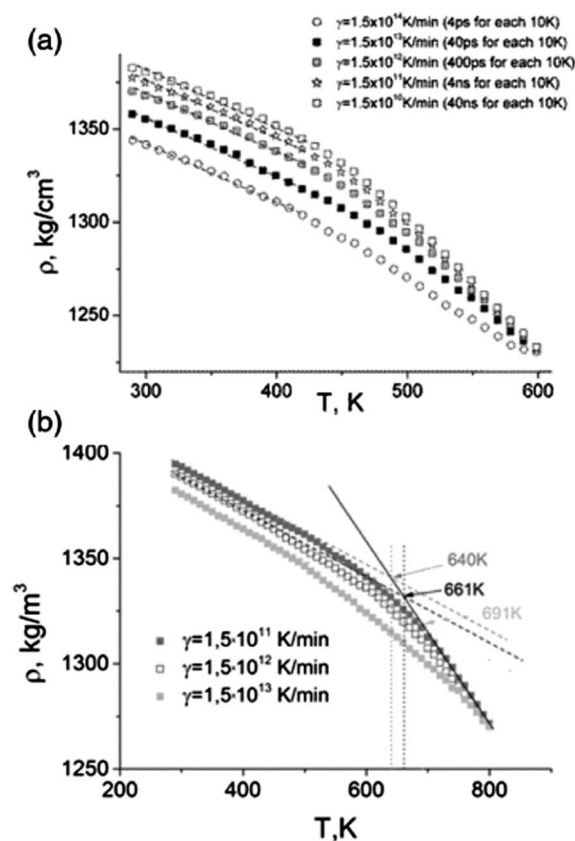


Fig. 4 The mass density of the R-BAPS polyimide as a function of temperature for the samples without (a) and with (b) partial charges with different cooling rates. Dashed lines indicate the same slope for all cooling rates in the low-temperature domain ( $T < T_g$ ) and vertical dotted lines serve as guide for the eye to define the  $T_g$  value at different cooling rates.

in simulations was estimated to be  $\sim 210$  °C or 483 K, see Fig. 3. As is evident from Fig. 4, the slope of the “density-temperature” curves in the low-temperature domain ( $T < T_g$ ) does not depend on the cooling rate, while the corresponding slope in the high-temperature domain ( $T > T_g$ ) is clearly cooling-rate dependent within the temperature range studied. As the slope of the “density-temperature” curves should not depend on the cooling rate, we conclude that the value of the cooling rate in MD simulations cannot be taken arbitrary: an appropriate value of the cooling rate should be chosen such that the slope of the “density-temperature” curves in the high-temperature domain ( $T > T_g$ ) would be cooling-rate insensitive. The wide range of slopes of the  $\rho(T)$  curves in the high-temperature domain may be related to the increase of the vitrification area induced by the combination of polyimide spatial mobility restrictions and extremely high cooling rate.

To verify this we carried out additional extensive simulations at higher temperatures for the systems with electrostatic interactions, with cooling starting from 800 K (all 11 samples were heated from 600 K to 800 K, equilibrated further during 100 ns and after that the electrostatic interactions were switched on) which require the use of smaller simulation time steps, namely, 1 fs, Fig. 4b. For these systems we obtained the  $\rho(T)$  dependence

for five cooling rates ( $\gamma = 1.5 \times 10^{11}$ ,  $7.5 \times 10^{11}$ ,  $1.5 \times 10^{12}$ ,  $7.5 \times 10^{12}$ ,  $1.5 \times 10^{13}$  K min<sup>-1</sup>) and calculated  $T_g$  values, Fig. 4b and 5. Smaller cooling rates are computationally too expensive as the electrostatic interactions in the system are handled with the use of the particle-mesh Ewald method, slowing down MD simulations by a factor of 3.<sup>45</sup>

Fig. 4 indicates that for the samples without electrostatic interactions the slope of  $\rho(T)$ -curves at  $T > T_g$  tends to reach saturation when the cooling rate approaches  $\gamma = 1.5 \times 10^{10}$  K min<sup>-1</sup>. However, to see whether such saturation is indeed achieved one has to perform the cooling of polyimide samples with an even slower rate of  $1.5 \times 10^9$  K min<sup>-1</sup> which is currently not feasible as it requires  $\sim 13$   $\mu$ s of MD simulations for each sample. As we demonstrate below, the dependence of the  $\rho(T)$ -curves at  $T > T_g$  on the cooling rate leads to uncertainty in evaluation of  $T_g$ .

For the samples with electrostatic interactions the slope of  $\rho(T)$ -curves at  $T > T_g$  are the same in the range 750–800 K at  $\gamma = 1.5 \times 10^{11}$  K min<sup>-1</sup> and  $\gamma = 1.5 \times 10^{12}$  K min<sup>-1</sup>, Fig. 4b.

The glass transition temperature was determined from the  $\rho(T)$ -curves as follows. The linear fit was applied to the  $\rho(T)$ -curves in the high-temperature domain ( $T > T_g$ ) and in the low-temperature domain ( $T < T_g$ ). The intersection of the two straight lines defined the glass transition temperature. The results are summarized in Fig. 5. In Fig. 5 we plot these values of  $T_g$  as a function of the cooling rate  $\gamma$ . As the cooling rate in MD simulations is several orders of magnitude larger than that in the experiment, the glass transition temperature measured in simulations is also larger. This effect has been well documented in a number of previous studies.<sup>25–28</sup> As seen from Fig. 5, the  $\gamma$ -dependence of  $T_g$  can be approximated by the logarithmic function of the well-known form<sup>29,36,39–41,62</sup>

$$T_g(\gamma) = T_0 - \frac{B}{\log(A\gamma)}, \quad (2)$$

where  $A$  and  $B$  are polymer-dependent constants and  $T_0 = 483$  K is the glass transition temperature at an infinitely slow (*i.e.*

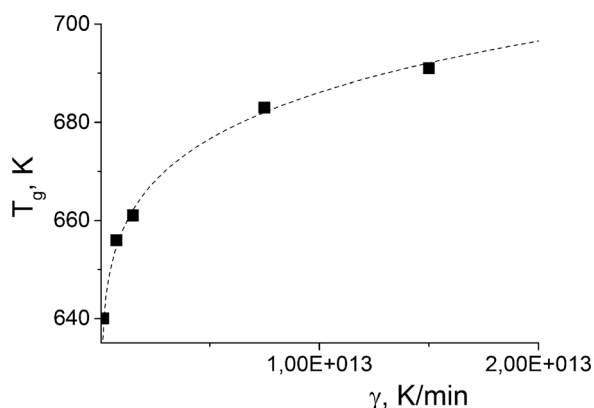


Fig. 5 The glass transition temperature *versus* cooling rate  $\gamma$  as measured from atomic-scale MD simulations (squares). Shown are the results for the R-BAPS samples with partial charges switched on. The solid line corresponds to fitting with the use of eqn (2) with the following set of parameters:  $A = 7.0 \times 10^{-20}$  min K<sup>-1</sup>,  $B = 1250$  K, and  $T_0 = 483$  K.

experimental) cooling rate which perfectly corresponds to the experimental value for the same molecular weight (see, Fig. 3). We note that the logarithmic dependence given by eqn (2) was reported in several computational studies, *e.g.* for amorphous polystyrene melts<sup>39</sup> where the cooling rate was varied in the range  $\gamma = 3 \times 10^{11}$  to  $6 \times 10^{13}$  K min<sup>-1</sup>.

Thus, our findings demonstrate that the calculation of  $T_g$  should be employed with great caution for verification of the polyimide computational models against experimental data: in addition to the well-known influence of the cooling rate on the glass-transition temperatures, correct definition of  $T_g$  in simulation depends not only on the method of calculation<sup>63</sup> but also requires cooling that starts from very high temperatures (no less than 800 K for considered polyimides) and evaluation of the appropriate cooling rate to make sure that the slope of the “density–temperature” curves in the high-temperature domain is insensitive to the cooling rate, otherwise the errors in the  $T_g$  evaluation become undefined.<sup>63</sup> Taken together, one can conclude that the glass transition temperature is not suitable for verification of computational models against experimental data since extremely high CPU resources are required. As we proceed to show in the next section, measuring the coefficient of thermal expansion of glassy polyimides provides a much more reasonable way to do such a verification.

The density–temperature curves for both polyimide samples with and without partial charges are shown in Fig. 6 (we note that the cooling rate was the same for both systems,  $\gamma = 1.5 \times 10^{11}$  K min<sup>-1</sup>). As seen from Fig. 6, switching the partial charges on leads to a remarkable increase in the glass transition temperature:  $T_g = 640$  K and  $T_g = 459$  K for the samples with and without electrostatic interactions, respectively.

The observed difference in the glass transition temperature can be understood in terms of strong intra- and intermolecular interactions in the system due to the presence of sulphone groups with relatively large partial charges: such interactions partly arrest mobility of the polyimide chains, so that the transition to the glassy state occurs at a higher temperature.<sup>38,42</sup>

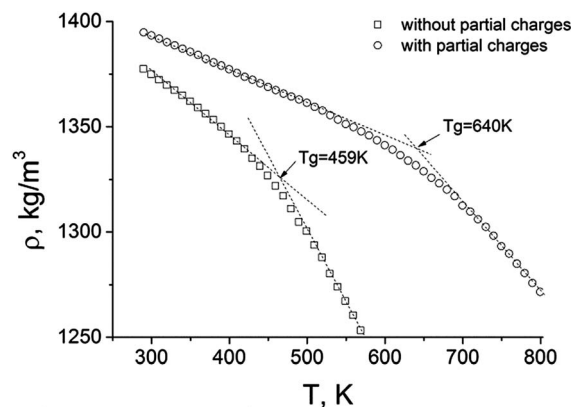


Fig. 6 The mass density of the R-BAPS polyimide as a function of temperature. Shown are the results for systems with (circles) and without (squares) partial charges. The cooling rate was set to  $\gamma = 1.5 \times 10^{11}$  K min<sup>-1</sup>.

### The coefficient of thermal expansion

Experimentally, the coefficient of linear thermal expansion, CLTE, was first measured with the use of linear dilatometry, see “Experimental methods” section for details. The temperature dependence of the volumetric coefficient of temperature expansion, CTE, was recalculated then from the CLTE. The experimental results are presented in Table 1.

On the computational side, the volumetric thermal expansion coefficient CTE can be calculated from the dependence of the sample volume (or the mass density) on temperature in the low-temperature domain ( $T < T_g$ ). At low temperatures the CTE is defined as

$$\text{CTE} = \frac{1}{V_0} \left( \frac{dV}{dT} \right)_p, \quad (3)$$

where  $V_0$  is the sample volume at a low temperature and  $(dV/dT)_p$  is the derivative of volume with respect to temperature at constant pressure. In other words, the CTE is defined by the slope of  $V(T)$ -curves at  $T < T_g$ . As demonstrated in the previous section, the slope of  $\rho(T)$ -curves (and correspondingly  $V(T)$ -curves) does not depend on the cooling rate in the low-temperature domain, see Fig. 4. Therefore, one can expect that CTE would be a much more reasonable characteristic for comparison with the experiment as compared to the glass transition temperature.

The dependence of the R-BAPS sample volume and of the CTE on temperature is shown in Fig. 7a for the samples with and without partial charges; the cooling rate was set to  $\gamma = 1.5 \times 10^{11} \text{ K min}^{-1}$ . The average values of the thermal expansion coefficient are given in Table 1 for both experiment and

**Table 1** The average values of CTE (from MD simulations and experiment) for the samples of R-BAPS and EXTEM™ polyimides with and without electrostatic interactions. The averaging is performed over the temperature range from 370 K to 410 K

	R-BAPS, $\text{K}^{-1}$	EXTEM™, $\text{K}^{-1}$
Experiment	$1.1 \times 10^{-4}$	$1.5 \times 10^{-4}$ (ref. [64])
MD simulations, partial charges are switched off	$2.6 \times 10^{-4}$	$2.1 \times 10^{-4}$
MD simulations, full electrostatics	$1.2 \times 10^{-4}$	$1.4 \times 10^{-4}$

computer simulations; the averaging was done over a rather narrow range of temperatures (370–410 K). It is seen that the computational value of CTE for the R-BAPS samples with full electrostatics is in very good agreement with experimental data, while the value of CTE for the samples with partial charges switched off is considerably overestimated, see Table 1. This is one of the key results of the present study. First of all, the excellent agreement with experiment verifies our computational R-BAPS polyimide model in general and its partial charges in particular. Second, our findings stress a crucial role of electrostatic interactions in thermal properties of heat-resistant polyimides with sulphone groups in their monomer units: setting the partial charges to zero leads to essentially incorrect theoretical predictions for the volumetric thermal expansion coefficient, see Table 1.

Remarkably, both conclusions are most likely of generic nature. To check this we repeated our simulations and CTE calculations for the commercial heat-resistant polyimide EXTEM™, another representative of polyimides with sulphone

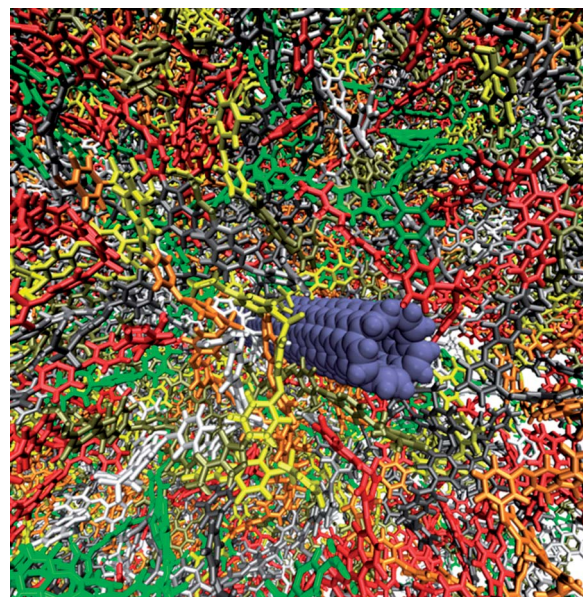


**Fig. 8** Snapshot of an equilibrated configuration (after 1.5  $\mu\text{s}$  of atomistic MD simulations) of a nanocomposite based on an R-BAPS polyimide and a single-wall carbon nanotube (colored by blue).

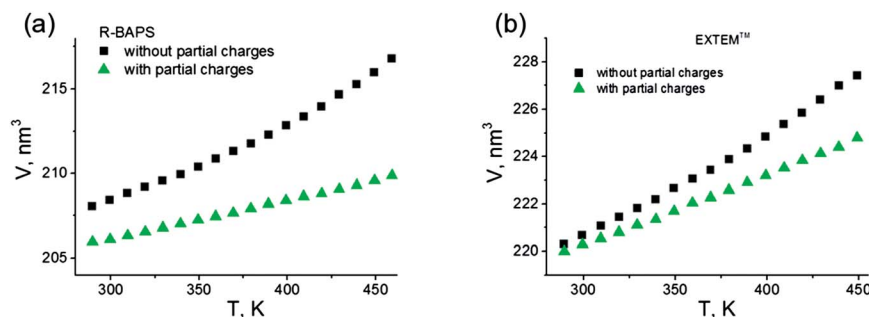


**Fig. 7** The sample volume as a function of temperature in the low-temperature domain ( $T < T_g$ ) for (a) R-BAPS and (b) EXTEM™ polyimide samples with and without electrostatic interactions (in both cases the cooling rate was set to  $\gamma = 1.5 \times 10^{11} \text{ K min}^{-1}$ ).



groups in the backbone, see Fig. 1 and “Computer simulation methods” section for the chemical structure of the monomer unit of EXTEM™ and for the details of simulations. The corresponding dependence of the EXTEM™ sample volume on temperature and the average values of CTE are presented in Fig. 7b and Table 1, respectively. Again, one can witness very good agreement between the results of MD simulations and of the experiment<sup>62</sup> when the electrostatic interactions in the system are properly accounted for.

The polyimide’s computational model validated extensively in this study along with developed simulation protocols is very promising for follow-up studies of thermoplastic nanocomposite materials. As an illustration of our ongoing simulation studies, in Fig. 8 we show a snapshot of a well-equilibrated composite sample based on the R-BAPS polyimide with a single-wall carbon nanotube as a filler. The results of these studies will be reported in our forthcoming publications.

## Conclusions

Polyimides represent a very important class of industrial polymer materials mostly due to their excellent heat-resistant properties. Therefore, theoretical models developed for polyimides have to reproduce their thermal properties as accurate as possible. In this study we employ a combination of experimental and computer modeling methods to identify a thermal characteristic to be preferably used for calibrating computational models *via* comparison with experimental data. For this purpose we chose R-BAPS, a polyimide with an oxidized sulphone group in the monomer unit. The presence of the sulphone group makes atomic-scale molecular dynamics simulations of the R-BAPS polyimide particularly challenging as polyimide’s partial charges are substantial and cannot be neglected.

Despite the fact that the glass transition temperature,  $T_g$ , is widely used for verification of theoretical models of glassy polymers, our findings clearly demonstrate that one should be careful to employ it for validation of MD simulations of polyimides. The main reason for that is in dramatic difference (up to 10 orders of magnitude) in cooling rates used in simulations and experiments, resulting in cooling-rate sensitivity of the computational value of  $T_g$ . What is more, the slope of the “density–temperature” curves in the high-temperature domain ( $T > T_g$ ) may also depend on the cooling rate making errors in the evaluation of undefined  $T_g$ . Moreover, the temperature of glass transition may depend on the method of its evaluation.<sup>62</sup> Therefore, when using the glass transition temperature for comparison of simulation results with experimental data, one has to make sure first that the slope of  $\rho(T)$ -curves is not cooling-rate dependent. We would like to mention another possible way for calculating the glass transition temperature of a polymer that does not involve cooling down with a pre-defined thermal routine. A typical representative of such methods is direct Monte Carlo simulations with a progressive decrease of temperature, which allows us to achieve system equilibration at any given  $T$ . In this case the calculated values of  $T_g$  correspond

to an infinitely slow cooling rate;<sup>65</sup> we plan to carry out such simulations in our forthcoming studies.

As an alternative to the glass transition temperature, we propose to use the coefficient of thermal expansion, CTE, for verification of computational models. This quantity is determined by the slope of the “volume–temperature” curve in the low-temperature domain ( $T < T_g$ ); the slope was shown to be insensitive to the cooling rate which allows us to overcome the cooling-rate related issues typical for the glass transition temperature. Indeed, our results for the coefficient of thermal expansion, being cooling-rate independent, agree very well with experimental data, verifying thereby the computational model developed for the R-BAPS polyimide.

Finally, we also demonstrated that partial charges are essential for a proper description of the R-BAPS polyimide: switching the charges off resulted in disagreement with experimental data on the coefficient of thermal expansion. This conclusion is most likely of generic nature and should hold for other polyimides with a similar chemical structure. In particular, we confirmed it for the commercial polyimide EXTEM™, another representative of polyimides with oxidized sulphone groups in the backbone.

## Acknowledgements

This study was carried out under the financial support of the Russian Ministry of Education and Science (State Agreements no. 8023 and no. 8645 and State Contract no. 16.523.12.3001 (Joint Russia-EU “COMPANOCOMP” project within the FP7 framework)) and megagrant of the Government of the Russian Federation, application 2013-220-04-006. The simulations have been performed using the computational resources of the Institute of Macromolecular Compounds, Russian Academy of Sciences, and the Chebyshev and Lomonosov supercomputers at Moscow State University.

## Notes and references

- 1 M. I. Bessonov, M. M. Koton, V. V. Kudryavtsev and L. A. Laius, *Polyimides – thermally stable polymers*, Consultants Bureau, New York, 1987.
- 2 M. J. M. Abadie and A. L. Rusanov, *Practical Guide to Polyimides*, Smithers Rapra Technology Limited, Shawbury, 2007.
- 3 V. E. Yudin and V. M. Svetlichnyi, *Russ. J. Gen. Chem.*, 2010, **80**, 2157.
- 4 V. E. Yudin, G. M. Divoux, J. U. Otaigbe and V. M. Svetlichnyi, *Polymer*, 2005, **46**, 10866.
- 5 S. Neyertz, *Soft Mater.*, 2007, **4**, 15.
- 6 J. Xia, S. Liu, P. K. Pallathadka, M. L. Chng and T. Chung, *Ind. Eng. Chem. Res.*, 2010, **49**, 12014.
- 7 R. Zhang and W. L. Mattice, *J. Membr. Sci.*, 1995, **108**, 15.
- 8 D. Hofmann, L. Fritz, J. Ulbrich and D. Paul, *Comput. Theor. Polym. Sci.*, 2000, **10**, 419.
- 9 S. Neyertz and D. Brown, *Macromolecules*, 2008, **41**, 2711.
- 10 M. Heuchel, D. Hofmann and P. Pullumbi, *Macromolecules*, 2004, **37**, 201.



- 11 C. Nagel, E. Schmidtke, K. Günther-Schade, D. Hofmann, D. Fritsch, T. Strunskus and F. Faupel, *Macromolecules*, 2000, **33**, 2242.
- 12 D. Hofmann, L. Fritz, J. Ulbrich, C. Schepers and M. Böhning, *Macromol. Theory Simul.*, 2000, **9**, 293.
- 13 O. Hölck, M. Heuchel, M. Böhning and D. Hofmann, *J. Polym. Sci., Part B: Polym. Phys.*, 2008, **46**, 59.
- 14 S. Neyertz, A. Douanne and D. Brown, *J. Membr. Sci.*, 2006, **280**, 517.
- 15 S. Neyertz, A. Douanne and D. Brown, *Macromolecules*, 2005, **38**, 10286.
- 16 S. Neyertz and D. Brown, *Macromolecules*, 2004, **37**, 10109.
- 17 S. Neyertz and D. Brown, *Macromolecules*, 2009, **42**, 8521.
- 18 S. Pandiyan, D. Brown, S. Neyertz and N. F. A. van der Vegt, *Macromolecules*, 2010, **43**, 2605.
- 19 S. Neyertz, D. Brown, S. Pandiyan and N. F. A. van der Vegt, *Macromolecules*, 2010, **43**, 7813.
- 20 S. Neyertz, *Macromol. Theory Simul.*, 2007, **16**, 513.
- 21 S. Velioglu, M. G. Ahunbay and S. B. Tantekin-Ersolmaz, *J. Membr. Sci.*, 2012, **418**, 217.
- 22 M. Minellia, M. G. De Angelisa and D. Hofmann, *Fluid Phase Equilib.*, 2012, **333**, 87.
- 23 L. Zhang, Y. Xiao, T.-S. Chung and J. Jiang, *Polymer*, 2010, **51**, 4439.
- 24 Y. Chen, S. P. Huang, Q. L. Liu, I. Broadwell and A. M. Zhu, *J. Appl. Polym. Sci.*, 2011, **120**, 1859.
- 25 Y. Chen, Q. L. Liu, A. M. Zhu, Q. G. Zhang and J. Y. Wu, *J. Membr. Sci.*, 2010, **348**, 204.
- 26 R. Pan, W. Zhao, T. Zhou and A. Zhang, *J. Polym. Sci., Part B: Polym. Phys.*, 2010, **48**, 595.
- 27 M. Li, X. Y. Liu, J. Q. Qin and Y. Gu, *eXPRESS Polym. Lett.*, 2009, **3**, 665.
- 28 D. Qi, J. Hinkley and G. He, *Modell. Simul. Mater. Sci. Eng.*, 2005, **13**, 493.
- 29 J. Buchholz, W. Paul, F. Varnik and K. Binder, *J. Chem. Phys.*, 2002, **117**, 7364.
- 30 K. Binder, J. Baschnagel and W. Paul, *Prog. Polym. Sci.*, 2003, **28**, 115.
- 31 J.-L. Barrat, J. Baschnagel and A. Lyulin, *Soft Matter*, 2010, **6**, 3430.
- 32 K. Binder, *Monte Carlo and Molecular Dynamics Simulations in Polymer Science*, Oxford University Press, USA, 1995.
- 33 B. Vorselaars, A. V. Lyulin and M. A. J. Michels, *Macromolecules*, 2007, **40**, 6001.
- 34 A. V. Lyulin, B. Vorselaars, M. A. Mazo, N. K. Balabaev and M. A. J. Michels, *Europhys. Lett.*, 2005, **71**, 618.
- 35 T. Liang, X. Yang and X. Zhang, *J. Polym. Sci., Part B: Polym. Phys.*, 2001, **39**, 2243.
- 36 K. Vollmayr, W. Kob and K. Binder, *J. Chem. Phys.*, 1996, **105**, 4714.
- 37 Y. Yani and M. H. Lamm, *Polymer*, 2009, **50**, 1324.
- 38 S. V. Lyulin, S. V. Larin, A. A. Gurtovenko, N. V. Lukasheva, V. E. Yudin, V. M. Svetlichnyi and A. V. Lyulin, *Polym. Sci., Ser. A*, 2012, **54**, 631.
- 39 A. V. Lyulin, N. K. Balabaev and M. A. J. Michels, *Macromolecules*, 2003, **36**, 8574.
- 40 A. Soldera and N. Metatla, *Phys. Rev. E: Stat., Nonlinear, Soft Matter Phys.*, 2006, **74**, 061803.
- 41 J. Baschnagel, K. Binder and H.-P. Wittmann, *J. Phys.: Condens. Matter*, 1993, **5**, 1597.
- 42 S. V. Lyulin, A. A. Gurtovenko, S. V. Larin, V. M. Nazarychev and A. V. Lyulin, *Macromolecules*, 2013, **46**, 6357.
- 43 C. Oostenbrink, A. Villa, A. E. Mark and W. F. van Gunsteren, *J. Comput. Chem.*, 2004, **25**, 1656.
- 44 A. A. Granovsky, *Firefly* version 7.1.G, <http://classic.chem.msu.su/gran/firefly/index.html>.
- 45 T. Darden, D. York and L. Pedersen, *J. Chem. Phys.*, 1993, **98**, 10089.
- 46 U. Essmann, L. Perera, M. L. Berkowitz, T. Darden, H. Lee and L. G. Pedersen, *J. Chem. Phys.*, 1995, **103**, 8577.
- 47 B. Hess, H. Bekker, H. J. C. Berendsen and J. G. E. M. Fraaije, *J. Comput. Chem.*, 1997, **18**, 1463.
- 48 H. J. C. Berendsen, in *Computer Simulations in Materials Science*, ed. M. Meyer and V. Pontikis, Kluwer, Dordrecht, 1991.
- 49 B. Hess, C. Kutzner, D. van der Spoel and E. Lindahl, *J. Chem. Theory Comput.*, 2008, **4**, 435.
- 50 D. van der Spoel, E. Lindahl, B. Hess, G. Groenhoff, A. E. Mark and H. J. C. Berendsen, *J. Comput. Chem.*, 2005, **26**, 1701.
- 51 V. A. Harmandaris, V. G. Mavrantzas and D. N. Theodorou, *Macromolecules*, 1998, **31**, 7934.
- 52 F. Müller-Plathe, *ChemPhysChem*, 2002, **3**, 754.
- 53 V. A. Harmandaris, D. Reith, N. F. A. van der Vegt and K. Kremer, *Macromol. Chem. Phys.*, 2007, **208**, 2109.
- 54 P. V. Komarov, C. Yu-Tsung, C. Shih-Ming, P. G. Khalatur and P. Reineker, *Macromolecules*, 2007, **40**, 8104.
- 55 S. V. Larin, S. G. Falkovich, V. M. Nazarychev, A. A. Gurtovenko, A. V. Lyulin and S. V. Lyulin, *RSC Adv.*, 2014, **4**, 830.
- 56 M. Mondello, H.-J. Yang, H. Furuya and R.-J. Roe, *Macromolecules*, 1994, **27**, 3566.
- 57 T. G. Fox and P. J. Flory, *J. Appl. Phys.*, 1950, **21**, 581.
- 58 V. M. Nazarychev, S. V. Larin, N. V. Lukasheva, A. D. Glova and S. V. Lyulin, *Polym. Sci., Ser. A*, 2013, **55**, 570.
- 59 P. J. Flory, *Statistical Mechanics of Chain Molecules*, Wiley, New-York, 1969.
- 60 P. J. Flory, *Macromolecules*, 1974, **7**, 381.
- 61 R. Zhang and W. Mattice, *Macromolecules*, 1993, **26**, 6100.
- 62 R. Brüning and K. Samwer, *Phys. Rev. B: Condens. Matter Mater. Phys.*, 1992, **46**, 11318.
- 63 A. R. C. Baljon, M. H. M. Van Weert, R. B. DeGraaff and R. Khare, *Macromolecules*, 2005, **38**, 2391.
- 64 Sabic Innovative Plastics™, <http://kbam.geampod.com/KBAM/Reflection/Assets/20311.pdf>.
- 65 O. Alexiadis, V. G. Mavrantzas, R. Khare, J. Beckers and A. R. C. Baljon, *Macromolecules*, 2008, **41**, 987.